

**\*\*Volume Title\*\***

*ASP Conference Series, Vol. \*\*Volume Number\*\**

**\*\*Author\*\***

© **\*\*Copyright Year\*\*** *Astronomical Society of the Pacific*

## Requirements for the Analysis of Quiet Sun Internetwork Magnetic Elements with EST and ATST

D. Orozco Suárez,<sup>1</sup> L.R. Bellot Rubio,<sup>2</sup> and Y. Katsukawa<sup>1</sup>

<sup>1</sup>*National Astronomical Observatory of Japan, 2-21-1 Osawa, Mitaka, Tokyo 181-8588, Japan*

<sup>2</sup>*Instituto de Astrofísica de Andalucía (CSIC), Apdo. de Correos 3004, 18080 Granada, Spain*

**Abstract.** The quiet Sun internetwork is permeated by weak and highly inclined magnetic fields whose physical properties, dynamics, and magnetic interactions are not fully understood. High spatial resolution magnetograms show them as discrete magnetic elements that appear/emerge and disappear/cancel continuously over the quiet Sun surface. The 4-m European Solar Telescope (EST) and the Advanced Technology Solar Telescope (ATST) will obtain two-dimensional, high cadence, high precision polarimetric measurements at the diffraction limit (30 km). Here, we compile the basic requirements for the observation of internetwork fields with EST and ATST (field of view, cadence, instrument configuration, etc). More specifically, we concentrate on the field-of-view requirements. To set them we analyze the proper motion of internetwork magnetic elements across the solar surface. We use 13 hours of magnetograms taken with the Hinode satellite to identify and track thousands of internetwork magnetic element in an isolated supergranular cell. We calculate the velocity components of each element and the mean distance they travel. The results show that, on average, magnetic elements in the interior of supergranular cells move toward the network. The radial velocity is observed to depend on the distance to the center of the supergranule. Internetwork magnetic elements travel 4'' on average. These results suggest that ATST and EST should cover, at least, one supergranular cell to obtain a complete picture of the quiet Sun internetwork.

### 1. Introduction: Properties of Quiet Sun Internetwork Magnetic Fields

Obtaining a clear picture of the solar magnetism and of the various physical processes taking place in the solar atmosphere strongly relies on the precise determination of the magnetic field vector. This is very true for the tiny magnetic structures that permeate the quieter areas of the solar photosphere, the so-called internetwork fields (IN; Livingston & Harvey 1975; Lites et al. 2008). Many of the physical properties of the IN fields have been inferred from the analysis of steady four-dimensional images ( $x$ ,  $y$ ,  $\lambda$ ,  $p$ )<sup>1</sup> constructed from spectropolarimetric measurements. For instance, IN observations taken with the spectropolarimeter (SP; Lites et al. 2001) of the 50-cm telescope on-board the Hinode satellite (Kosugi et al. 2007) show that IN magnetic fields are weak and have large inclinations to the local vertical (e.g., Orozco Suárez & Bellot Rubio

---

<sup>1</sup>Two spatial dimensions, wavelength, and four polarization states (Stokes I, Q, U, and V).

2012). However, even at the best spatial resolution achieved so far in the IN ( $0''.15$  with SUNRISE/IMaX, Barthol et al. 2011; Martínez Pillet et al. 2011), the amplitude of the polarization signals are very small and thus exposed to harmful noise effects. Moreover, the magnetic structures are still partially unresolved. Recent inversions of Stokes profiles indicate that the magnetic fill fractions in the IN are about 20% at  $0''.3$  resolution (Orozco Suárez et al. 2007). Also, observations show that the number and size of magnetic structures increase monotonically as the resolution improves (de Wijn et al. 2008; Danilovic et al. 2010; Ishikawa & Tsuneta 2010). On theoretical grounds, it is expected that magnetic structures will exist up to the resistivity scales of the solar plasma (a few meters, e.g., de Wijn et al. 2009 and Pietarila Graham et al. 2009).

In addition, the magnetic fields of the IN are highly dynamic and evolve through several physical processes such as emergence and cancellation. However, it is difficult to study their evolution using high-cadence raster scans from a spectropolarimeter. The reason is that to one needs exposures of a few seconds per slit position to achieve a polarimetric sensitivity of, say,  $10^{-3}I_c$  (or  $s/n \sim 1000$ )<sup>2</sup>. Therefore, the measurements have to be limited to very narrow regions of the solar surface, and even so the achievable cadence is of the order of minutes. Using this technique, it has been possible to characterize dynamic properties of magnetic flux emergence processes (e.g., Orozco Suárez et al. 2008; Martínez González & Bellot Rubio 2009). However, most of the dynamic properties of the IN fields have been determined from filter-based polarimeters which allow the observation of large fields of view at high cadence, but with far less spectral purity. From these measurements we know that the mean lifetime of IN magnetic elements is about 10 minutes, although it is difficult to set a mean lifetime for the polarization signals at high resolution (e.g., Danilovic et al. 2010). The rms fluctuation of the horizontal velocity of IN magnetic elements is  $1.57 \text{ km s}^{-1}$  (de Wijn et al. 2008). A drawback of filter-based instruments is that the physical information extracted from the observed polarization signals is often less accurate than that inferred from slit-based polarimeters because the data are affected by the modest spectral resolution and coarse wavelength sampling (Orozco Suárez et al. 2010).

Finally, the limited spatial resolution impedes the investigation of small-scale physical processes like reconnections, jets, or cancellations taking place in the quiet Sun IN. For instance, recent analyses of cancellation events observed in the IN with the Hinode spectropolarimeter show evidence of insufficient temporal and spatial resolution to “catch” the important physics behind these events (see e.g., Kubo et al. 2010). An example of a magnetic cancellation is shown in Fig. 1 using Na I 589.6 nm magnetograms acquired with the Narrowband Filter Imager of Hinode at a spatial resolution of about  $0''.3$ . The cancellation takes place in a very narrow region, right between the two magnetic elements, in the so-called polarity inversion line. Present spectropolarimetric measurements lack enough spatial resolution to observe cancellation boundaries in detail. In summary, the observation of IN fields by spectropolarimetric means is a very demanding task, but necessary to determine the physical properties of the quiet Sun.

Large photon collecting surfaces will improve both the photometric accuracy and the cadence of the measurements (Collados 2008; del Toro Iniesta & Orozco Suárez 2010), as well as the spatial resolution. Thus, it will be easier to determine the magnetic field vector from the observed polarization signals because the changes in the

---

<sup>2</sup>The signal-to-the-noise ratio ( $s/n$ ) is calculated in the continuum of Stokes I.

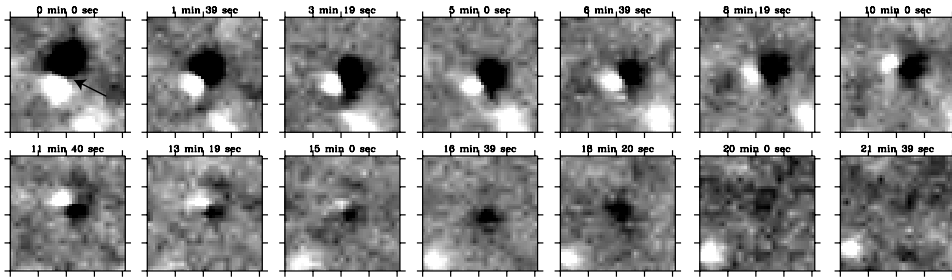


Figure 1. Magnetograms recorded with Hinode’s Narrowband Filter Imager showing the cancellation of two IN magnetic elements (left to right and top to bottom). The total duration of the sequence is about 22 minutes. The arrow pinpoints the cancellation site or polarity inversion line that is very small compared to the size of the canceling magnetic elements. Note how the magnetic elements rotate clockwise while the amplitude of the signals diminishes, suggesting that important dynamics may take place during the cancellation. Tick marks are separated by  $1''$ .

Stokes profile shapes resulting from variations of the physical quantities will be less influenced by the noise (e.g., del Toro Iniesta & Pillet 2011). In addition, the amplitude of the polarization signals will be greater since the magnetic filling factors tend to increase as the spatial resolution improves. By the same token, however, resolution also challenges the observation of extended areas of the solar surface at high cadence using spectropolarimeters, because of the large number of steps in the slit scan direction needed to cover significant fields of view. The European Solar Telescope (EST; Collados et al. 2010) and the Advanced Technology Solar Telescope (ATST; Keil et al. 2010) will be equipped with 4m mirrors, thus facilitating the measurement of quiet Sun IN field. Both will provide the photons needed to achieve high polarimetric accuracy and temporal resolution with small exposure times<sup>3</sup>.

In this contribution we aim at listing the main requirements for observing quiet Sun internetwork fields with EST and ATST using the current understanding about the magnetic and dynamic properties of IN magnetic elements. We put special attention on the fields of view needed to get a complete picture of the quiet Sun internetwork magnetism and of the physical processes taking place there.

## 2. Velocities of Internetwork Magnetic Elements and Traveled Distance

To set up limits on the field of view (FOV) to be observed by EST and ATST one can use the typical velocities (i.e., proper motions) and lifetimes (or traveled distances) of IN magnetic elements as a reference. If we are interested in analyzing individual magnetic features from birth (emergence/submergence or appearance of flux) to death (cancellation or disappearance), these two quantities may help constrain the required FOV because they inform us about the mean distance traveled by the magnetic elements in the solar surface. Most measurements concur that IN flux concentrations show two distinct velocity components: one of random nature, resulting from the continual buffeting of the fields by granular convection (e.g., Manso Sainz et al. 2011), and a net

<sup>3</sup>For details, see <http://www.est-east.eu> and <http://atst.nso.edu>

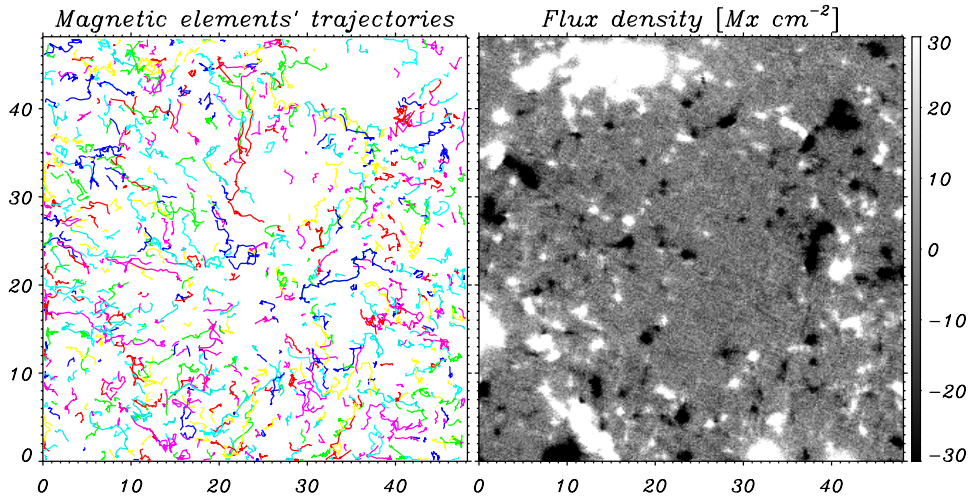


Figure 2. Right: Quiet Sun magnetogram taken with Hinode’s Narrowband Filter Imager, saturated at  $\pm 30$  G. The FOV covers one supergranular cell. Left: trajectories of some of the several thousand magnetic elements detected in 13 hours of magnetograms. The trajectories are more linear in the inner part and more random near the borders. Colors distinguish individual objects. Axis units are arcsec.

velocity that transports the fields from the center of supergranular cells toward their boundaries, i.e., toward the network. We are interested in the latter. However, while there exist robust estimations of the random velocity component, about  $1.57 \text{ km s}^{-1}$ , the values given in the literature for the net velocity range from  $0.2 \text{ km s}^{-1}$  (de Wijn et al. 2008) to  $0.35 \text{ km s}^{-1}$  (Zirin 1987). Only Zhang et al. (1998) investigated the spatial dependence of the velocity pattern of IN elements and found a constant radial velocity (measured from the center of supergranular cells outwards) of about  $0.4 \text{ km s}^{-1}$  using low resolution ( $1''.5$ ) and low cadence (7 min) magnetograms.

Here, we employ very high spatial resolution ( $0''.3$ ) Na I 589.6 nm magnetograms acquired by Hinode to estimate the net velocity component of IN magnetic elements. The magnetograms have a cadence of 80 seconds and a FOV of approximately  $93'' \times 82''$ , so they cover a few supergranular cells. The noise is 6.7 G. To analyze the data we first selected a small area of  $50'' \times 50''$  containing one supergranular cell and the network around it. Then we detected and tracked the proper motion of each magnetic element in consecutive magnetograms. In total, we analyzed 13 hours of data. For detecting and tracking magnetic elements we used the YAFTA\_10 software<sup>4</sup> (Yet Another Feature Tracking Algorithm; DeForest et al. 2007). In the detection process we ignored all magnetic elements with fluxes below 10 G and sizes smaller than  $16 \text{ px}^2$ .

The right panel of Figure 2 depicts a single  $50'' \times 50''$  snapshot extracted from the magnetogram time sequence. It contains a supergranular cell. One can clearly see large circular polarization signals concentrated at the borders of the image, corresponding to large flux values (i.e., network fields). In the inner part of the image there are flux elements that show opposite polarities and much smaller sizes than those associated with the network. These signals correspond to internetwork magnetic fields. The left

<sup>4</sup>YAFTA\_10 can be downloaded from <http://solarmuri.ssl.berkeley.edu/~welsch/public/software/YAFTA>

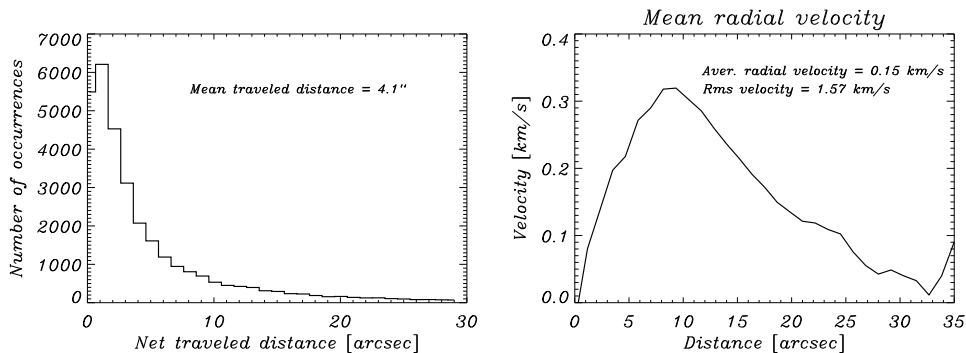


Figure 3. Left: histogram of the mean linear distance traveled by internetwork magnetic elements. The average value is  $4''.1$ . Right: Variation of the azimuthally averaged radial velocity component of the magnetic elements as a function of distance (position) from the center of the supergranule.

panel shows the paths of some of the several thousand elements detected and tracked in the magnetograms by YAFTA\_10. The paths of the elements located in the inner part of the supergranule are rather linear and radially aligned with respect to the center of the image. In the network, the paths “look” more random and show little linear trends. This figure alone suggests that quiet Sun magnetic elements have two distinct velocity components, one random and one systematic, both weighted differently depending on the location of the element within the supergranular cell.

Once we have the positions of each magnetic element in each of the magnetograms, we derive their horizontal velocities  $\mathbf{v} = (v_x, v_y)$ . Because there is a clear radial symmetry in the trajectory pattern we decided to translate the horizontal velocities into the radial  $v_R = \mathbf{v} \cdot \mathbf{r}/|\mathbf{r}|$  and transversal  $v_T = |\mathbf{r} \times \mathbf{v}|/|\mathbf{r}|$  components with respect to the center of the supergranular cell. Here the quantity  $\mathbf{r}$  stands for the displacement and  $v_R$  is measured positive outwards. Using the network at a reference, the supergranule center can be located at  $(x_c, y_c) \sim (26''.6, 22''.1)$ , i.e., very close to the center of the magnetogram displayed in Figure 2. Next we calculated the azimuthally averaged values of the radial velocity component as a function of distance from the center. We also calculated the mean linear distance  $|\overline{\mathbf{r}}|$  traveled by the magnetic elements detected by the tracking algorithm.

The results are shown in Fig. 3 for the average radial velocity (right panel) and the mean traveled distance (left panel). Interestingly, the radial component of the velocity shows a dependence with the distance to the supergranular cell center. The magnetic elements close to the center are almost at rest. The radial velocity increases outwards until it reaches a maximum value of  $0.32 \text{ km s}^{-1}$  at  $9''$  from the supergranular center. Then, it decreases monotonically. We find a mean radial velocity of  $0.15 \text{ km s}^{-1}$ , slightly smaller than previous estimations (de Wijn et al. 2008; Zirin 1987; Zhang et al. 1998). Overall, the magnetic elements move toward the network. These results indicate that the dynamic properties of the quiet Sun magnetic elements are different depending on their location within the supergranular cell.

The histogram for the mean traveled distance shows a peak at small values and has an extended tail that reaches  $20''$ . This implies that most magnetic elements travel small distances, although some of them can get as far as half the diameter of a typical supergranular cell. The mean traveled distance is  $4''.1$ . It is important to keep in mind

that during the tracking process we did not take into account the fact that small magnetic elements tend to collide with others during their trip to the network. Such collisions give rise to splitting of signals, merging of signals of the same polarity, and cancellation of signals of opposite polarity. Such interactions create “new” elements in the sense that the signals change their properties enough to make the tracking algorithm interpret them as new magnetic elements. Hence, the mean distance is being underestimated and the value given here should be considered a lower limit.

### 3. Summary: Minimum Requirements to Observe IN Magnetic Fields

In this section we compile the minimum requirements for observing quiet Sun IN fields with ATST and EST. With their 4m mirrors, these telescopes will collect 64 times more photons than 50-cm telescopes (if we assume the same photon efficiency), which will alleviate most of the current limitations encountered in the study of quiet Sun IN fields.

- *Spatial resolution*: On average, we know that the fill fraction is about 20% for 120 km ( $0''.16$ ) pixel size (e.g., Orozco Suárez et al. 2007). Thus, we need to increase the spatial resolution up to 30 km (the diffraction limit of ATST and EST at 500 nm) to spatially resolve them.
- *Temporal resolution*: a minimum time cadence may be given by the rms velocity of the magnetic elements and the spatial resolution. Assuming a rms velocity of  $1.5 \text{ km s}^{-1}$  (measured with a 1-meter class telescope) and a spatial resolution of 30 km, the magnetic elements would take about 20 seconds to move from one pixel to the next. We shall set half of this time as the minimum cadence for critical sampling of the motions in the case of diffraction-limited observations. Note that since the measured rms velocity increases with spatial resolution, a cadence of 10 seconds may be severely underestimated. In addition, the rms velocity of the magnetic elements also poses limitations for the exposure times that should be much smaller than 10 seconds to prevent image degradation. If we take the sound speed in the photosphere (about  $8 \text{ km s}^{-1}$ ) as a reference, then all measurements have to be performed about five times faster, i.e., in about two seconds. The high cadence will allow the study of fast physical phenomena like cancellation events.
- *Polarization sensitivity*: The number of photons collected per resolution element is independent of the telescope diameter at the diffraction limit (see e.g., Keller (2003)). For this reason, 4-meter telescopes will have the same polarization sensitivity as 50-centimeter telescopes, provided the photon efficiency is maintained. Thus, taking the exposure times of the Hinode spectropolarimeter as a reference, at the diffraction limit ATST and EST will reach a s/n ratio of  $\sim 1000$  with integration times of five seconds. For the quiet Sun internetwork we need to go beyond noise levels of  $10^{-3} I_c$ . Thus, there are two options: increase the exposure time or downgrade the spatial resolution. For instance, we can reach  $2.5 \times 10^{-4} I_c$  with five second exposure times and  $0''.1$  resolution. Note that since it is expected that the polarization signals will be larger because of the increased resolution, it may be possible to fully characterize the IN fields with s/n  $\sim 1000$ . Thus, a better option may be to achieve a s/n of 1000 in less than a few tenths of a second at  $0''.1$  spatial resolution.

- *Field of view*: Which FOV is most appropriate for the study of quiet Sun magnetic fields? To investigate the dynamics and interactions between magnetic elements, a FOV covering a minimum area of 4'' seems necessary. However, we have seen that there exist clear connections between the dynamics and the spatial location within supergranular cells. Therefore, the observation of a complete supergranule (about 30'' diameter) would be highly desirable.

Is it possible for ATST and EST to meet all the above requirements? With slit-based instruments only, the answer is negative. The reason is that the spatial resolution of the observations should be kept close to the diffraction limit of ATST and EST to advance our understanding of IN magnetic fields. Hinode observations have shown that a spatial resolution of 0'.3 is not enough to characterize the magnetic processes taking place in the IN. But, at the diffraction limit of a 4-meter telescope ( $\sim 0'.05$ ), it takes more than six minutes for a spectrograph to scan a 4''-wide area with a  $s/n \sim 1000$ . Six minutes is far above the minimum requirements set by the current observations. One can make a compromise and reduce the spatial resolution to about 0'.1, but it would still take about 1.5 minutes to scan the same area maintaining the  $s/n$ .

Therefore, systems capable of scanning a given FOV while maintaining the polarimetric sensitivity and temporal resolution seem necessary if one wants to fulfill the minimum requirements to characterize internetwork fields, study their dynamics, and analyze the physical processes in which they participate. These are, for instance, multi-slit configurations, image slicing instruments, or fiber optics arrays (see e.g., Socas-Navarro 2010). In particular, the latter concept has been successfully implemented in the SpectroPolarimetric Imager for the Energetic Sun (SPIES), an instrument which observes 2D FOVs without compromising the spatial, temporal, or spectral resolution (see Lin, this volume).

Another option is to use tunable filters instead of spectrographs. However, although filtergraph observations can achieve noise levels close to  $10^{-3}$  (e.g., Martínez Pillet et al. 2011) and the determination of the magnetic field vector is possible from such observations (e.g., Orozco Suárez et al. 2010), the uncertainties of the physical quantities inferred from these instruments are larger than those derived from spectropolarimetric measurements. Among other reasons, this is due to the fact that the shapes of the spectral lines are strongly distorted by the passband of filter-based polarimeters and the long times needed to scan the spectral line.

**Acknowledgments.** D.O.S. thanks the Japan Society for the Promotion of Science (JSPS) for financial support through the postdoctoral fellowship program for foreign researchers. Hinode is a Japanese mission developed and launched by ISAS/JAXA, with NAOJ as domestic partner and NASA and STFC (UK) as international partners. It is operated by these agencies in co-operation with ESA and NSC (Norway).

## References

- Barthol, P., et al. 2011, *Solar Phys.*, 268, 1  
 Collados, M. 2008, *Lecture Notes and Essays in Astrophysics*, 3, 113  
 Collados, M., Bettonvil, F., Cavaller, L., Ermolli, I., Gelly, B., Pérez, A., Socas-Navarro, H., Soltau, D., Volkmer, R., & EST team 2010, *Astronomische Nachrichten*, 331, 615  
 Danilovic, S., Beeck, B., Pietarila, A., Schüssler, M., Solanki, S. K., Martínez Pillet, V., Bonet, J. A., del Toro Iniesta, J. C., Domingo, V., Barthol, P., Berkefeld, T., Gandorfer, A., Knölker, M., Schmidt, W., & Title, A. M. 2010, *ApJ*, 723, L149

- de Wijn, A. G., Lites, B. W., Berger, T. E., Frank, Z. A., Tarbell, T. D., & Ishikawa, R. 2008, *ApJ*, 684, 1469
- de Wijn, A. G., Stenflo, J. O., Solanki, S. K., & Tsuneta, S. 2009, *Space Sci.Rev.*, 144, 275
- DeForest, C. E., Hagenaar, H. J., Lamb, D. A., Parnell, C. E., & Welsch, B. T. 2007, *ApJ*, 666, 576
- del Toro Iniesta, J. C., & Orozco Suárez, D. 2010, *Astronomische Nachrichten*, 331, 558
- del Toro Iniesta, J. C., & Pillet, V. M. 2011, in *IAU Symposium*, vol. 273 of *IAU Symposium*, 37
- Ishikawa, R., & Tsuneta, S. 2010, *ApJ*, 718, L171
- Keil, S. L., Rimmele, T. R., Wagner, J., & ATST team 2010, *Astronomische Nachrichten*, 331, 609
- Keller, C. U. 2003, in *Society of Photo-Optical Instrumentation Engineers (SPIE) Conference Series*, edited by S. Fineschi, vol. 4843 of *Society of Photo-Optical Instrumentation Engineers (SPIE) Conference Series*, 100
- Kosugi, T., Matsuzaki, K., Sakao, T., Shimizu, T., Sone, Y., Tachikawa, S., Hashimoto, T., Minesugi, K., Ohnishi, A., Yamada, T., Tsuneta, S., Hara, H., Ichimoto, K., Suematsu, Y., Shimojo, M., Watanabe, T., Shimada, S., Davis, J. M., Hill, L. D., Owens, J. K., Title, A. M., Culhane, J. L., Harra, L. K., Doschek, G. A., & Golub, L. 2007, *Solar Phys.*, 243, 3
- Kubo, M., Low, B. C., & Lites, B. W. 2010, *ApJ*, 712, 1321
- Lites, B. W., Elmore, D. F., & Ständer, K. V. 2001, in *Advanced Solar Polarimetry – Theory, Observation, and Instrumentation*, edited by M. Sigwarth, vol. 236 of *Astronomical Society of the Pacific Conference Series*, 33
- Lites, B. W., Kubo, M., Socas-Navarro, H., Berger, T., Frank, Z., Shine, R., Tarbell, T., Title, A., Ichimoto, K., Katsukawa, Y., Tsuneta, S., Suematsu, Y., Shimizu, T., & Nagata, S. 2008, *ApJ*, 672, 1237
- Livingston, W. C., & Harvey, J. 1975, in *Bulletin of the American Astronomical Society*, vol. 7 of *Bulletin of the American Astronomical Society*, 346
- Manso Sainz, R., Martínez González, M. J., & Asensio Ramos, A. 2011, *A&A*, 531, L9
- Martínez González, M. J., & Bellot Rubio, L. R. 2009, *ApJ*, 700, 1391
- Martínez Pillet, V., Del Toro Iniesta, J. C., Álvarez-Herrero, A., Domingo, V., Bonet, J. A., González Fernández, L., López Jiménez, A., Pastor, C., Gasent Blesa, J. L., Mellado, P., Piqueras, J., Aparicio, B., Balaguer, M., Ballesteros, E., Belenguer, T., Bellot Rubio, L. R., Berkefeld, T., Collados, M., Deutsch, W., Feller, A., Girela, F., Grauf, B., Heredero, R. L., Herranz, M., Jerónimo, J. M., Laguna, H., Meller, R., Menéndez, M., Morales, R., Orozco Suárez, D., Ramos, G., Reina, M., Ramos, J. L., Rodríguez, P., Sánchez, A., Uribe-Patarroyo, N., Barthol, P., Gandorfer, A., Knoelker, M., Schmidt, W., Solanki, S. K., & Vargas Domínguez, S. 2011, *Solar Phys.*, 268, 57
- Orozco Suárez, D., & Bellot Rubio, L. R. 2012, *ApJ*, 749, in press
- Orozco Suárez, D., Bellot Rubio, L. R., del Toro Iniesta, J. C., & Tsuneta, S. 2008, *A&A*, 481, L33
- Orozco Suárez, D., Bellot Rubio, L. R., del Toro Iniesta, J. C., Tsuneta, S., Lites, B. W., Ichimoto, K., Katsukawa, Y., Nagata, S., Shimizu, T., Shine, R. A., Suematsu, Y., Tarbell, T. D., & Title, A. M. 2007, *ApJ*, 670, L61
- Orozco Suárez, D., Bellot Rubio, L. R., Martínez Pillet, V., Bonet, J. A., Vargas Domínguez, S., & Del Toro Iniesta, J. C. 2010, *A&A*, 522, A101+
- Pietarila Graham, J., Danilovic, S., & Schüssler, M. 2009, *ApJ*, 693, 1728
- Socas-Navarro, H. 2010, *Astronomische Nachrichten*, 331, 581
- Zhang, J., Lin, G., Wang, J., Wang, H., & Zirin, H. 1998, *A&A*, 338, 322
- Zirin, H. 1987, *Solar Phys.*, 110, 101